Taylor & Francis
Taylor & Francis Group

Mechanics Based Design of Structures and Machines

An International Journal

ISSN: 1539-7734 (Print) 1539-7742 (Online) Journal homepage: https://www.tandfonline.com/loi/lmbd20

Synthesis of a novel planar linkage to visit up to eight poses

Henry Alberto Suárez-Velásquez, J. Jesús Cervantes-Sánchez & José M. Rico-Martínez

To cite this article: Henry Alberto Suárez-Velásquez, J. Jesús Cervantes-Sánchez & José M. Rico-Martínez (2018) Synthesis of a novel planar linkage to visit up to eight poses, Mechanics Based Design of Structures and Machines, 46:6, 781-799, DOI: 10.1080/15397734.2018.1483829

To link to this article: https://doi.org/10.1080/15397734.2018.1483829

MECHANICS BASED DESIGN OF STRUCTURES AND MACHINES
2018, VOL. 46, NO. 6, 781–799
https://doi.org/10.1080/15397734.2018.1483829

Synthesis of a novel planar linkage to visit up to eight poses

Henry Alberto Suárez-Velásquez, J. Jesús Cervantes-Sánchez, and José M. Rico-Martínez

Departamento de Ingeniería Mecánica, DICIS, Universidad de Guanajuato, Guanajuato, México

ABSTRACT

This article introduces a novel planar linkage which results from combining a Wanzer linkage with a four-bar linkage. It has one degree of freedom and is able to visit exactly up to eight poses. The proposed design approach yields linkages without branch and order defects, which can move continuously between all the desired poses without disassembly. Three illustrative examples show the applicability and the validity of the proposed synthesis process.

ARTICLE HISTORY
Received 8 December 2017
Accepted 30 May 2018

KEYWORDS
Exact synthesis; motion generation; Wanzer linkage; planar four-bar linkage; finite poses; branching analysis

1. Introduction

The kinematic design of planar linkages with only one degree of freedom is still a subject of current research interest (Sancibrian et al., 2012; Venkataramanujam and Larochelle, 2015; Akgün, 2016; Gezgin et al., 2016; Kumar et al., 2017).

When the desired task requires to visit a number of finite poses, which is lesser or equal to five, then we can use a planar four-bar linkage (Schröcker et al., 2005; Brunnthaler et al., 2006; Ge et al., 2013). Other examples of exact synthesis for five finite poses on a plane include also a six-bar Stephenson mechanism (Schreiber et al., 2002), or a Watt-I six-bar linkage (Soh and McCarthy, 2008).

To perform a task that requires to visit exactly more than five poses, it is necessary to search for linkages with more advanced motion capabilities (Chen and Angeles, 2008). To this end, it is proposed in this article, a novel linkage that is able to visit up to eight poses exactly. This novel linkage has only one degree of freedom, and it resulted from the combination of a Wanzer linkage with a four-bar linkage. To the best of our knowledge, all the studies of the Wanzer linkage that appear in the literature have been focused on its kinematic analysis and type synthesis (Uicker et al., 2017), and no attention has been given to consider it as a motion generator device. Thus, in the first part of this article, there are developed the synthesis equations for the Wanzer linkage, which showed that it is a very limited motion generation device. In the second part of the article, the modified Wanzer linkage is analyzed. It includes a comprehensive branching analysis. This analysis serves to test design candidates in order to avoid design failures, such as branch, order, and circuit defects. As a result, the proposed design approach may be used to synthesize linkages without branch defect, which can move continuously between all the desired poses without disassembly. Examples of successful designs are provided.

CONTACT J. Jesús Cervantes-Sánchez jecer@ugto.mx Departamento de Ingeniería Mecánica, DICIS, Universidad de Guanajuato, Salamanca, Guanajuato 36885, Mexico.
Color versions of one or more of the figures in the article can be found online at www.tandfonline.com/lmbd.

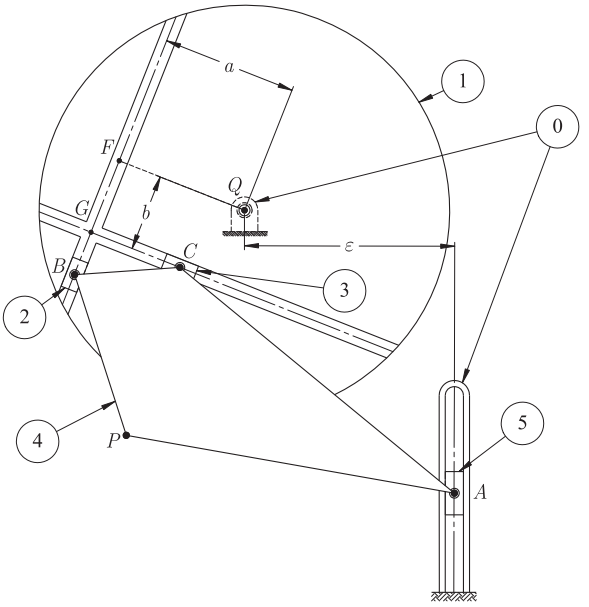

Figure 1. The Wanzer linkage.

2. The Wanzer linkage

The Wanzer mechanism has only one degree of freedom, and it is composed of five moving links (links 1–5), and one fixed body, link 0, see Fig. 1.

It is important to mention that link 4 will be considered as the *coupler link* of the Wanzer linkage, and it will be used to reach all prescribed poses.

2.1. Finite poses of the coupler link

Figure 2 shows the coupler link in two finitely separated poses, namely, pose 0, and arbitrary pose *i*. The guided body is represented by a trapezoidal block, which is assumed to be attached to and move with the coupler of the linkage.

It is required to design the linkage such that the guided body visits exactly a set of finitely separated poses, which are given con respect to the first pose, namely pose 0, as $\{p_i, \phi_i\}_0^n$, with $\phi_i \equiv \beta_i - \beta_0$.

2.2. Constraint equations

The design parameters a, b, and ε, are shown in Figs. 1 and 3, lead to the obtaining of three constraint equations whose derivation is based on the geometry shown in Fig. 2.

2.2.1. First constraint equation

The first constraint equation is related to the geometrical parameter a, see Figs. 1 and 2, which can be computed at any pose as follows:

$$\left(r_{B_i/P_0} - r_{Q/P_0}\right) \cdot v_i = a = \left(r_{B_0/P_0} - r_{Q/P_0}\right) \cdot v_0, \quad i = 1, 2, ..., n, \tag{1}$$

where

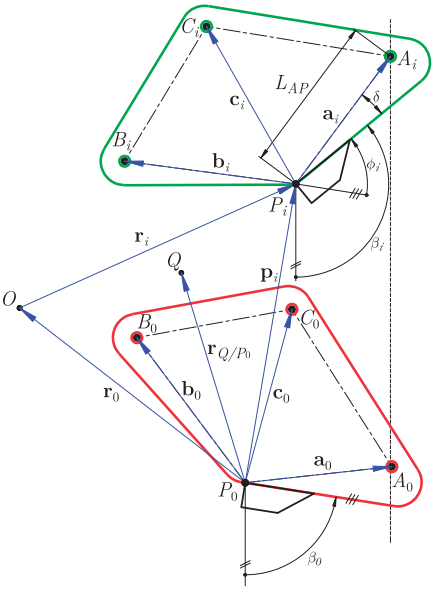

Figure 2. The prescribed poses and the coupler link.

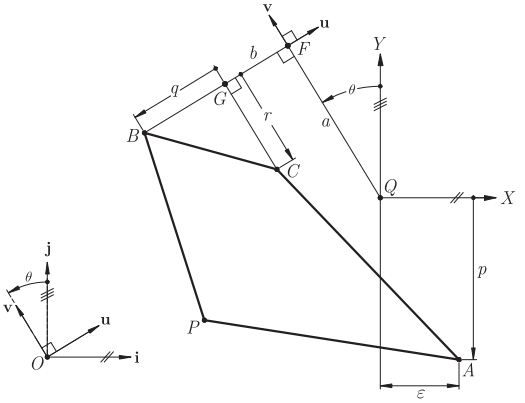

Figure 3. Geometry of the Wanzer linkage.

$$
\begin{aligned}
r_{B_0/P_0} &= x_B i + y_B j \equiv b_0,\\
r_{Q/P_0} &= x_Q i + y_Q j,\\
v_0 &= -\sin\theta_0 i + \cos\theta_0\ j,\\
v_i &= -\sin\theta_i i + \cos\theta_i\ j,\\
r_{B_i/P_0} &= p_i + R_{0\to i} b_0,\\
p_i &= x_i i + y_i j,\\
R_{0\to i} &= \begin{bmatrix} \cos\phi_i & -\sin\phi_i \\ \sin\phi_i & \cos\phi_i \end{bmatrix}.
\end{aligned}
$$

Being $R_{0\to i}$ a matrix which serves to rotate vector b_0, from 0-th pose, to vector b_i, at i-th pose, i.e., $b_i = R_{0\to i} b_0$, and, hereafter, $r_{k/j}$ will denote the position vector of point k with respect to point j. Thus, after some algebraic manipulation, Eq. (1) becomes:

$$-(x_B-x_Q)\sin\theta_0+(y_B-y_Q)\cos\theta_0+(x_i-x_Q+x_B\cos\phi_i-y_B\sin\phi_i)\sin\theta_i- \\ -(y_i-y_Q+x_B\sin\phi_i+y_B\cos\phi_i)\cos\theta_i=0,\quad i=1,2,\ldots,n. \tag{2}$$

Which is the first constraint equation sought.

2.2.2. Second constraint equation

The second constraint equation involves now the geometrical parameter b, see Figs. 1 and 2, which is given by:

$$(r_{Q/P_0}-r_{C_i/P_0})\cdot u_i=b=(r_{Q/P_0}-r_{C_0/P_0})\cdot u_0,\quad i=1,2,\ldots,n, \tag{3}$$

where, in addition to those mathematical expressions previously described for Eq. (1), we have now that:

$$r_{C_0/P_0}=x_Ci+y_Cj\equiv c_0,$$
$$u_0=\cos\theta_0 i+\sin\theta_0\ j,$$
$$u_i=\cos\theta_i i+\sin\theta_i\ j,$$
$$r_{C_i/P_0}=p_i+R_{0\to i}c_0.$$

Then, after some algebraic manipulation, Eq. (3) becomes

$$(x_C-x_Q)\cos\theta_0+(y_C-y_Q)\sin\theta_0-(y_i-y_Q+x_C\sin\phi_i+y_C\cos\phi_i)\sin\theta_i- \\ -(x_i-x_Q+x_C\cos\phi_i-y_C\sin\phi_i)\cos\theta_i=0,\quad i=1,2,\ldots,n. \tag{4}$$

Which is the second constraint equation sought.

2.2.3. Third constraint equation

The geometrical parameter ε shown in Figs. 1 and 2 lead to the formulation of the third constraint equation. To this end, the design parameter ε can be computed as follows:

$$(r_{A_i/P_0}-r_{Q/P_0})\cdot i=\varepsilon=(r_{A_0/P_0}-r_{Q/P_0})\cdot i,\quad i=1,2,\ldots,n, \tag{5}$$

where, in addition to those mathematical expressions previously described for Eqs. (1) and (3), we have now that:

$$r_{A_0/P_0}=x_Ai+y_Aj\equiv a_0,$$
$$r_{A_i/P_0}=p_i+R_{0\to i}a_0.$$

Thus, after some algebraic manipulation, Eq. (5) becomes

$$x_A(\cos\phi_i-1)-y_A\sin\phi_i+x_i=0,\quad i=1,2,\ldots,n. \tag{6}$$

Which is the third constraint equation sought.

2.3. Analysis of the constraint equations

The main objective of the synthesis process is to compute the design parameters of the linkage. Hence, those variable parameters related to the displacements of the links are not of interest for the designer. This is the case of angle θ_i that appears in Eqs. (2) and (4), which represents the rotation of the slotted disk 1 at the i -th pose. Then, angle θ_i can be eliminated as follows. Solving Eqs. (2) and (4) for $\sin\theta_i$ and $\cos\theta_i$, and substituting the values obtained into the trigonometric identity $\sin^2\theta_i+\cos^2\theta_i=1$, yields:

$$(h_{1i}k_{20}-k_{10}h_{2i})^2+(k_{10}g_{2i}+g_{1i}k_{20})^2-(g_{1i}h_{2i}+h_{1i}g_{2i})^2=0, i=1,2,\ldots,n, \tag{7}$$

Table 1. Constraint equations, unknowns, and number of poses.

Equation	Unknowns	Involved poses	Maximum number of poses
(6)	x_A, y_A	0, 1, 2	3
(16)	x_B, y_B, x_C, y_C, x_Q, y_Q, θ_0	0,1,2, … ,7	8

where

$$g_{1i} \equiv x_i - x_Q + x_B \cos\phi_i - y_B \sin\phi_i. \tag{8}$$

$$h_{1i} \equiv y_i - y_Q + x_B \sin\phi_i + y_B \cos\phi_i. \tag{9}$$

$$k_{10} \equiv -(x_B - x_Q)\sin\theta_0 + (y_B - y_Q)\cos\theta_0. \tag{10}$$

$$g_{2i} \equiv y_i - y_Q + x_C \sin\phi_i + y_C \cos\phi_i. \tag{11}$$

$$h_{2i} \equiv x_i - x_Q + x_C \cos\phi_i - y_C \sin\phi_i. \tag{12}$$

$$k_{20} \equiv (x_C - x_Q)\cos\theta_0 + (y_C - y_Q)\sin\theta_0. \tag{13}$$

Going further, after substitution of the corresponding coefficients g_{ji}, h_{ji}, and $k_{j0}, j = 1, 2$, Eq. (7) becomes:

$$\Psi_{1i}\cos^2\theta_0 + \Psi_{2i}\sin\theta_0\cos\theta_0 + \Psi_{3i}\sin^2\theta_0 + \Psi_{4i} = 0. \tag{14}$$

where coefficients $\Psi_{1i}, \Psi_{2i}, \Psi_{3i}$, and Ψ_{4i} depend on the pose data, x_i, y_i, ϕ_i, as well as on the unknown design parameters x_B, y_B, x_C, y_C, x_Q, y_Q.

Equation (14) can be further simplified if we resort to the following double-angle trigonometric identities:

$$\cos^2\theta_0 = \frac{1}{2}(1 + \cos 2\theta_0), \quad \sin\theta_0\cos\theta_0 = \frac{1}{2}\sin 2\theta_0, \quad \sin^2\theta_0 = \frac{1}{2}(1 - \cos 2\theta_0). \tag{15}$$

Thus, Eq. (14) becomes:

$$(\Psi_{1i} - \Psi_{3i})\cos 2\theta_0 + \Psi_{2i}\sin 2\theta_0 + \Psi_{1i} + \Psi_{3i} + 2\Psi_{4i} = 0, \quad i = 1, 2, \ldots, n. \tag{16}$$

It should be noted that Eq. (14) is quadratic in terms of $\sin\theta_0$ and $\cos\theta_0$, whereas Eq. (16) is linear in terms of $\sin 2\theta_0$ and $\cos 2\theta_0$. Thus, the order of the equation under study has been reduced from two to one. This is important when solving nonlinear trigonometric equations.

Summarizing, constraint Eqs. (2) and (4) have been combined into one single equation, i.e., Eq. (16). Hence, only two mathematical tools remain for the design of the Wanzer linkage, namely, Eqs. (6) and (16). At this point, it is very important to realize that, due to the adequate definition of the prescribed poses, both Eqs. (6) and (16) have implicitly involved the first given pose, that is, the 0-th pose. Moreover, these equations have a certain number of unknown parameters, and they are valid for a number of poses, as it is shown in Table 1.

3. Conception of the modified Wanzer linkage

Table 1 shows that the maximum number of prescribed poses that the coupler link 4 of the original Wanzer linkage could visit precisely is three, which is limited by the constraint Eq. (6). This constitutes a serious drawback to use the original Wanzer linkage as an effective motion generator device.

3.1. The modified Wanzer linkage

Constraint Eq. (6) is only valid for the original Wanzer linkage, and it represents a kinematic chain of the PR type, where symbol P stands for a prismatic joint, whereas symbol R denotes a revolute joint. Moreover, this PR chain joins the coupler link 4, with the fixed link 0, see Fig. 1. As it may be seen in Table 1, the PR chain limits drastically the number of poses to be visited,

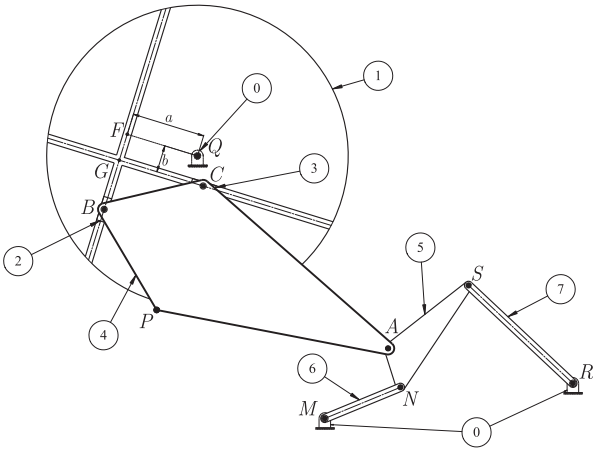

Figure 4. The modified Wanzer linkage.

since it constrains the motion of point A to be on a fixed line, see Fig. 1. Then, it is reasonable to think in substituting the PR chain for other kinematic chain such that the coupler link 4 may visit more than three poses. It should be noted that prismatic joints can be treated as special case of revolute joints in kinematic synthesis (Angeles and Bai, 2005).

From the foregoing discussion, a successful substitution of the PR chain could be achieved by using a planar four-bar linkage in a way that point A traces a continuous path on a plane, thus eliminating the straight-line motion constraint. On this regard, it is well known that a four-bar linkage can be synthesized for up to nine precision points in path generation tasks (Suh and Radcliffe, 1978).

On the other hand, it is interesting to mention that another possible modification is to consider that trammel's slides are not at right angles. This feature adds a new design parameter (the angle between slides) into the design process. However, it does not solve the limitation related to the reduced number of poses imposed by constraint equation (6).

As a result of the foregoing discussion, it was conceived the kinematic structure of the modified Wanzer linkage, as it may be seen in Fig. 4.

One may realize that the modified Wanzer linkage preserves a considerable part of the kinematic architecture of the original Wanzer linkage, except for the replacement of the PR chain by the planar four-bar linkage. This results in an increment of the number of links, from six to eight, and, as it will be shown later, the number of poses visited precisely will be incremented from three to eight. This is an important achievement from the point of view of kinematic design. It should be noted that according to the Chebyshev-Grübler-Kutzbach criterion, the modified Wanzer linkage shown in Fig. 4 still has one single degree of freedom (DOF).

4. Dimensional synthesis of the modified Wanzer linkage

The synthesis problem is now reduced to: (a) solve Eq. (16) for the eight given poses of the conducted body, and (b) constrain the motion of point A to be on the coupler curve of a four-bar linkage. Moreover, since Eq. (16) is already available, only remains to constrain the motion of point A. This is addressed in the following sections.

4.1. Synthesis of the rotatory trammel linkage

The so-called *rotatory trammel linkage* will be composed of links 0, 1, 2, 3, and 4, see Fig. 1. This linkage can be synthesized by solving the constraint Eq. (16), which can be written in a more compact form as follows:

$$(\Psi_{1i}-\Psi_{3i})\cos 2\theta_0 + \Psi_{2i}\sin 2\theta_0 + \Gamma_i = 0, \qquad \Gamma_i \equiv \Psi_{1i} + \Psi_{3i} + 2\Psi_{4i}, \qquad i = 1, 2, ..., 7. \tag{17}$$

Then, the objective is to solve Eq. (17) for the six design parameters x_B, y_B, x_C, y_C, x_Q, y_Q, and also for the secondary unknown θ_0. Once known these seven unknowns, the offsets a and b may be computed by means of Eqs. (1) and (3), respectively.

Additionally, as a byproduct of the foregoing procedure, the designer will be able to know the location of points B, C, and P of the coupler link 4, see Fig. 1. Therefore, only remains to compute the location of point A in order to complete the geometry of coupler link 4. To this end, the designer has the freedom to choose arbitrarily: (a) angle δ, and (b) length L_{AP}, see Fig. 2. Then, the location of point A of the coupler 4 can be computed for any given pose

$$r_{A_i/P_0} = p_i + L_{\mathrm{AP}}\sin(\beta_i + \delta)i - L_{\mathrm{AP}}\cos(\beta_i + \delta)j, \qquad p_0 = 0, \qquad i = 0, 1, 2, ..., 7. \tag{18}$$

It should be noted that the rotatory trammel linkage is itself a two degree of freedom linkage, and point A can move on a plane.

4.2. Synthesis of the planar four Bar linkage

The function of the planar four-bar linkage is to guide point A to visit exactly eight locations, $A_0, A_1, ..., A_7$, one for each prescribed pose, as it is illustrated in Fig. 5. Hence, it is required to perform a path generation task.

4.2.1. The coupler curve

Suárez-Velásquez (2018) developed a symbolic equation for the coupler curve to be followed by point A of the four-bar linkage shown in Fig. 5, which is given by

$$(\mu_{1i}\lambda_{22i} - \mu_{2i}\lambda_{12i})^2 + (-\mu_{1i}\lambda_{21i} + \mu_{2i}\lambda_{11i})^2 - (\lambda_{11i}\lambda_{22i} - \lambda_{12i}\lambda_{21i})^2 = 0, \qquad i = 0, 1, 2, ..., 8, \tag{19}$$

where

$$\begin{aligned}
\lambda_{11i} &\equiv -2g(x_M - x_{Ai}) + 2e(y_M - y_{Ai}).\\
\lambda_{12i} &\equiv 2e(x_M - x_{Ai}) + 2g(y_M - y_{Ai}).\\
\lambda_{21i} &\equiv -2g(x_N - x_{Ai}) - 2f(y_N - y_{Ai}).\\
\lambda_{22i} &\equiv -2f(x_N - x_{Ai}) + 2g(y_N - y_{Ai}).\\
\mu_{1i} &\equiv L_{\mathrm{MR}}^2 + 2x_{Ai}x_M + 2y_{Ai}y_M - x_{Ai}^2 - y_{Ai}^2 - x_M^2 - y_M^2 - e^2 - g^2.\\
\mu_{2i} &\equiv L_{\mathrm{NS}}^2 + 2x_{Ai}x_N + 2y_{Ai}y_N - x_{Ai}^2 - y_{Ai}^2 - x_N^2 - y_N^2 - f^2 - g^2.
\end{aligned}$$

With:

$$r_{Ai/P_0} = \begin{bmatrix} x_{Ai} \\ y_{Ai} \end{bmatrix}, \qquad r_{M/P_0} = \begin{bmatrix} x_M \\ y_M \end{bmatrix}, \qquad r_{N/P_0} = \begin{bmatrix} x_N \\ y_N \end{bmatrix}.$$

And L_{MR}, L_{NS}, e, f, and g, are the geometric parameters shown in Fig. 5. A different derivation of Eq. (19) can be found in Bai (2014), which resulted from a synthesis approach with incomplete data set.

4.2.2. The synthesis approach

Equation (19) must be valid for any pose reached by the modified Wanzer linkage, and also for the four-bar linkage to be designed. It involves nine unknowns, namely, x_M, y_M, x_N, y_N, L_{MR}, L_{NS}, e, f, and g. In consequence, Eq. (19) could be applied up to nine precision points. However, since

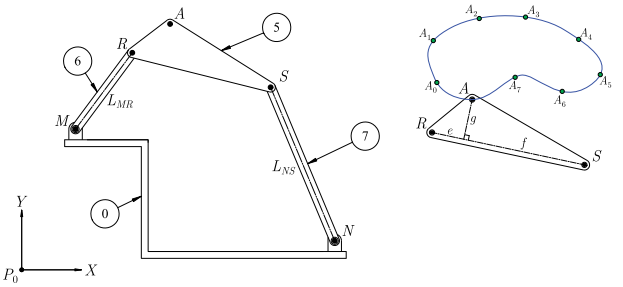

Figure 5. The planar four-bar linkage.

the design Eq. (17) of the rotatory trammel is only valid for eight poses, then Eq. (19) will be used only for eight locations, $A_0, A_1, ..., A_7$.

5. Synthesis for six, seven, and eight poses

Equations (17) and (19) can be used to design a modified Wanzer linkage to reach six, seven, and eight given poses. Table 2 shows details related to the design parameters, free parameters, and the number of poses to be reached.

The selection of the free parameters shown in Table 2 is based on the experience acquired after solving many examples. Thus, we found that these free parameters yield the best economy of computation. The free choice of several design parameters provides the designer the opportunity to obtain a virtually infinite number of solutions that could yield a larger number of successful designs.

6. Branching analysis

In general, a linkage may have two or more branches. Branching occurs when a linkage can be assembled in more than one configuration for a given configuration of the input link. Hence, each assembly mode is known as *branch*. For purposes of branching analysis related to the modified Wanzer linkage, the input link will be arbitrarily chosen as link 6, see Figs. 4 and 5.

6.1. Branches of the four bar linkage

Based on a position analysis of the four-bar linkage, see Fig. 5, the output variable η_3 (rotation of link 7) can be obtained in closed form in terms of the input variable η_1 (rotation of link 6) by means of the following quadratic equation:

$$(F_3 - F_1)\kappa^2 + 2F_2\kappa + (F_3 + F_1) = 0, \quad \kappa \equiv \tan\left(\frac{\eta_3}{2}\right), \tag{20}$$

where F_1, F_2, and F_3 depend on input angle η_1 and the linkage dimensions. Then the two roots of Eq. (20) produce the following conjugate output values:

Table 2. Design parameters, free parameters, and number of poses

Equation	Design parameters	Free parameters	Number of poses
(17)	x_B, y_B, y_C, x_Q, y_Q.	x_C, θ_0	6
(19)	x_M, x_N, L_{MR}, L_{NS}, e, f	y_M, y_N, g	6
(17)	x_B, y_B, x_C, y_C, x_Q, y_Q	θ_0	7
(19)	x_M, y_M, x_N, L_{MR}, L_{NS}, e, f	y_N, g	7
(17)	x_B, y_B, x_C, y_C, x_Q, y_Q, θ_0	None	8
(19)	x_M, y_M, x_N, y_N, L_{MR}, L_{NS}, e, f	g	8

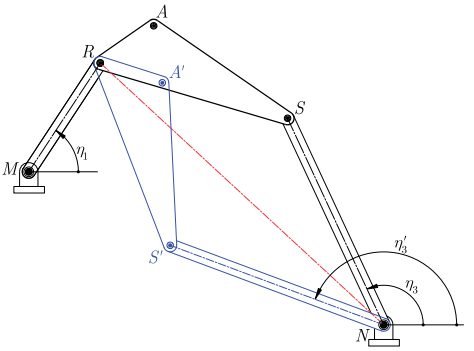

Figure 6. The two branches of the planar four-bar linkage.

$$\kappa_{1,2} = \frac{-F_2 \pm \sqrt{\Delta_\kappa}}{F_3 - F_1}, \quad \Delta_\kappa \equiv F_1^2 + F_2^2 - F_3^2. \tag{21}$$

Each output value of $\eta_3 = 2\arctan(\kappa)$ associated with Eq. (21) defines a conjugate configuration of the linkage. Since each branch corresponds to one particular sign in Eq. (21), the problem of branching can be eliminated by choosing one single sign of that equation. Thus, for a given orientation of the input link, one may get the two branches shown in Fig. 6.

6.2. Branches of the rotatory trammel linkage

Based on a position analysis of the rotatory trammel linkage, see Fig. 3, it is possible to obtain the following input-output equation:

$$\mathrm{Y}^4 + H_3\mathrm{Y}^3 + H_2\mathrm{Y}^2 + H_1\mathrm{Y} + H_0 = 0, \quad \mathrm{Y} \equiv \tan\left(\frac{\theta}{2}\right), \tag{22}$$

where coefficients H_0, H_1, H_2, and H_3 depend on input motions x_A, y_A, and the geometric parameters of the linkage. According to Beyer (1991), solving quartic Eq. (22) yields four conjugate solutions for the output angle θ, which are given by

$$\mathrm{Y}_{1,2} = -\left(\frac{1}{4}\right)H_3 + \left(\frac{1}{2}\right)R_1 \pm \left(\frac{1}{2}\right)R_2 \tag{23}$$

$$\mathrm{Y}_{3,4} = -\left(\frac{1}{4}\right)H_3 - \left(\frac{1}{2}\right)R_1 \pm \left(\frac{1}{2}\right)R_3, \tag{24}$$

where parameters R_1, R_2, and R_3 depend on coefficients H_0, H_1, H_2, and H_3 of the quartic Eq. (22). Each output value of $\theta_i = 2\arctan(\mathrm{Y}_i)$ associated with Eqs. (23) and (24) defines a branched configuration of the linkage. Since each branch corresponds to one particular sign in Eqs. (23) and (24), the problem of branching can be eliminated by choosing one single sign of these equations (Kohli et al., 1994). Thus, for a given position of point A, one may get the four branches shown in Fig. 7.

On the other hand, the discriminant Δ_Q of Eq. (22) is used to identify the *locking configuration* of a linkage (Kohli et al., 1994). This is mathematically defined as follows (Burnside and Panton, 1886):

$$\Delta_Q \equiv I^3 - 27J^2. \tag{25}$$

where

$$I \equiv h_0 - 4h_3h_1 + 3h_2^2,$$

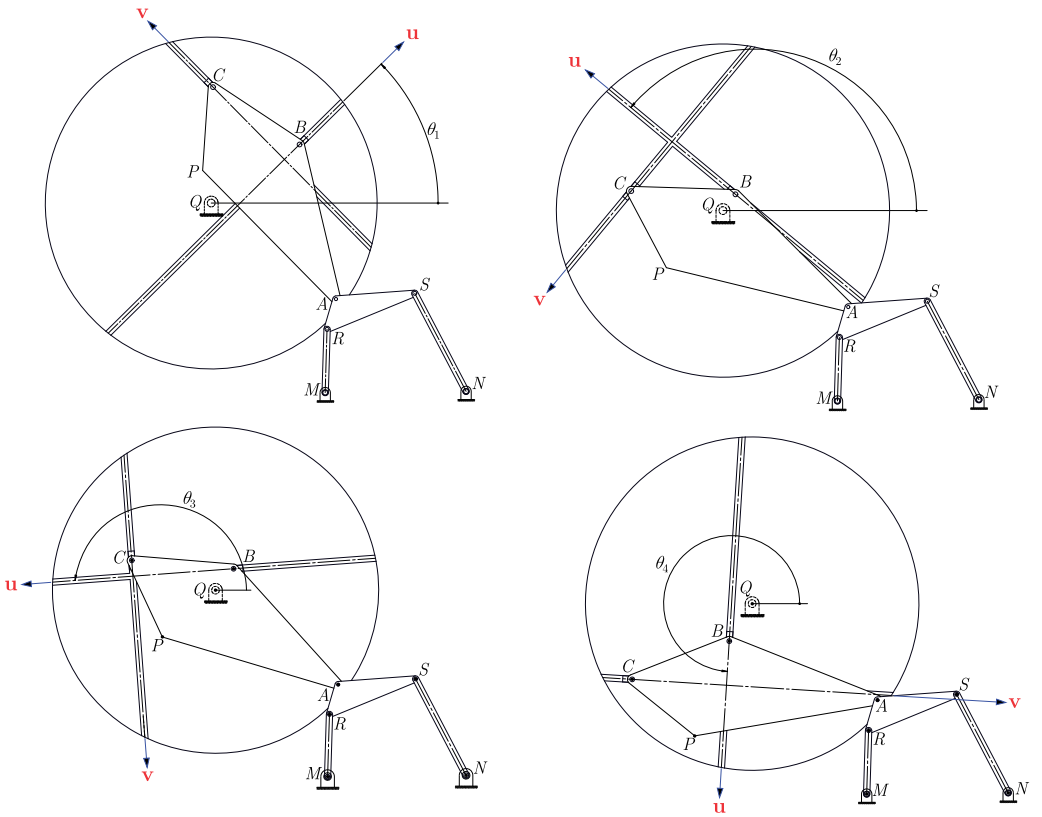

Figure 7. Branches of the rotatory trammel linkage.

$$J \equiv h_2h_0 + 2h_3h_2h_1 - h_1^2 - h_0h_3^2 - h_2^3,$$
$$h_3 \equiv \frac{H_3}{4}, h_2 \equiv \frac{H_2}{6}, h_1 \equiv \frac{H_1}{4}, h_0 \equiv H_0.$$

6.3. Total number of branches

It was previously shown that the four-bar linkage has two branches. Additionally, it was also proved that the rotatory trammel linkage has four assembly modes. Therefore, the whole modified Wanzer linkage will have up to eight possible configurations for any given orientation of link 6, that is, eight possible branches may be found for a general configuration of the complete linkage.

7. Criterion for a successful design

Once one solution is obtained, the corresponding design candidate has to be analyzed to evaluate their kinematic performance. The criterion for a successful design is that the coupler link reaches all, prescribed points P_i, as well as computed points A_i, for $i = 1, 2, \ldots, n$, following a prescribed order on a single trajectory, without passing through a locking configuration. Thus, the designed linkage will not have to be disassembled and reassembled in order for it to reach all the desired poses. Therefore, the designed linkage will have a continuous motion through the given poses. On the one hand, when the foregoing points cannot be reached on a single trajectory, it is said that the linkage under analysis has a *circuit defect* (Plecnik and McCarthy, 2016). On the other hand, if the design candidate must pass through a locking configuration to reach all the points, then

Table 3. Computational algorithm to synthesize a modified Wanzer linkage

Computational algorithm	
Parameters	Equations–figures
1. Prescribed poses: $\{p_i, \phi_i\}_0^7$	Given, see Fig. 2
2. Compute design parameters: x_B, y_B, x_C, y_C, x_Q, y_Q, and unknown θ_0	See Eq. (17)
3. Compute design parameter a	Equation (1)
4. Compute design parameter b	Equation (3)
5. Choose numerical values for length L_{AP} and angle δ	See Fig. 2
6. Compute the locations of point A, $r_{Ai/P_0} = (x_{Ai}, y_{Ai})^T$	See Eq. (18) and Fig. 2
7. Choose a suitable numerical value for the design parameter g	See Fig. 5
8. Compute design parameters: x_M, y_M, x_N, y_N, L_{MR}, L_{NS}, e, and f	See Eq. (19) and Fig. 5
9. Test for branching and locking configurations	See Eqs. (21)–(25)

Table 4. Poses for the examples.

Pose	0	1	2	3	4	5	6	7
X_i	0.00	0.45	1.32	2.29	2.88	2.95	2.60	1.93
Y_i	0.00	0.24	0.42	0.17	−0.43	−0.97	−1.26	−1.57
β_i	90.00°	77.36°	55.03°	30.20°	10.03°	1.71°	10.03°	30.20°

the design has what is known as *a branch defect* (Chase and Mirth, 1993; Balli and Chand, 2002). Locking configurations are those points where (a) the discriminant Δ_κ of Eq. (20) is equal to zero, and (b) the discriminant Δ_Q of the quartic equation (22) is equal to zero (Kohli et al., 1994).

8. Computational algorithm

A systematic solution procedure for the planar eight-pose synthesis problem of the modified Wanzer linkage is outlined in Table 3.

The idea of Table 3 is to provide the reader with a quick guide of the main stages to synthesize the modified Wanzer linkage. The extension to the synthesis for six or seven poses is straightforward. To this end, Table 2 shows more details.

9. Numerical examples

This section presents three detailed examples related to the dimensional synthesis of modified Wanzer linkages to visit exactly six, seven, and eight poses proposed by Prof. McCarthy (2002), see Table 4.

9.1. First example

In this example, the modified Wanzer linkage has to visit the first six poses shown in Table 4. Application of the computational algorithm shown in Table 3 yields the design parameters presented in Table 5. A 3D layout of the resulting linkage is shown in Fig. 8.

Table 5. Design parameters for the first example.

Parameter	Numerical value	Parameter	Numerical value
x_B	1.9791	x_M	−0.6476
y_B	0.2393	y_M	0.6000
x_C	0.0000	x_N	−2.3886
y_C	−0.6422	y_N	−3.2500
x_Q	1.3258	e	0.6259
y_Q	−1.8860	f	2.4334
θ_0	0.0000°	L_{AP}	2.0000
a	−2.1252	δ	240°
b	1.3258	g	1.8000
L_{MR}	1.0570	L_{NS}	2.2288

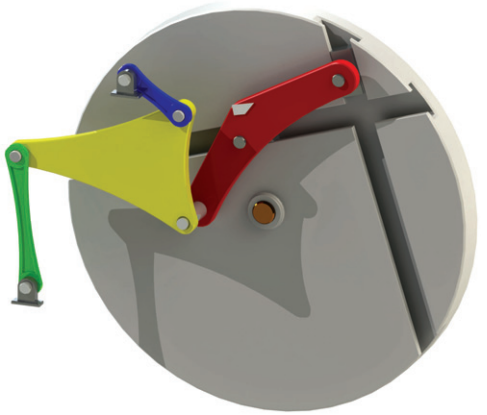

Figure 8. Resulting linkage for the first example.

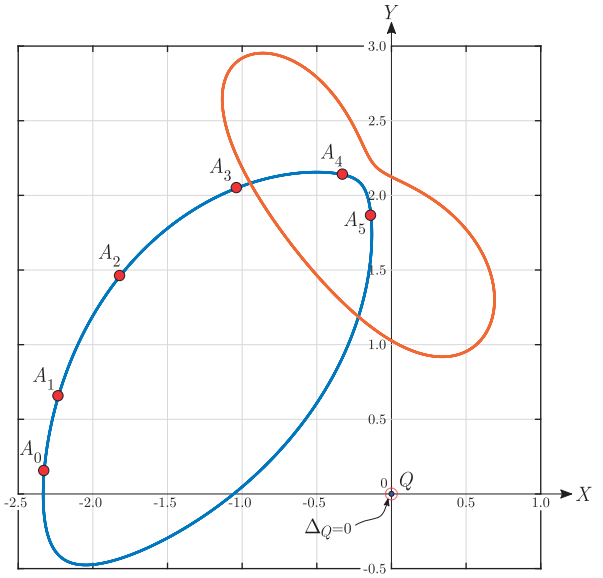

Figure 9. Coupler curves of the four-bar linkage for the first example.

The maximum synthesis error (round-off error) in this first example is 1.5×10^{-10} for the position of point P, and 3.5×10^{-6} degrees in the orientation of the guided body.

9.1.1. Evaluation of the performance of the first example

Analyzing the results shown in Figs. 9–11, we conclude that the resulting linkage is free of branch and order defect, and it can move continuously between all the desired poses without disassembly. Therefore, this is a successful design.

9.2. Second example

This second example consists in designing a modified Wanzer linkage whose coupler link moves exactly through the first seven poses shown in Table 4. Application of the computational

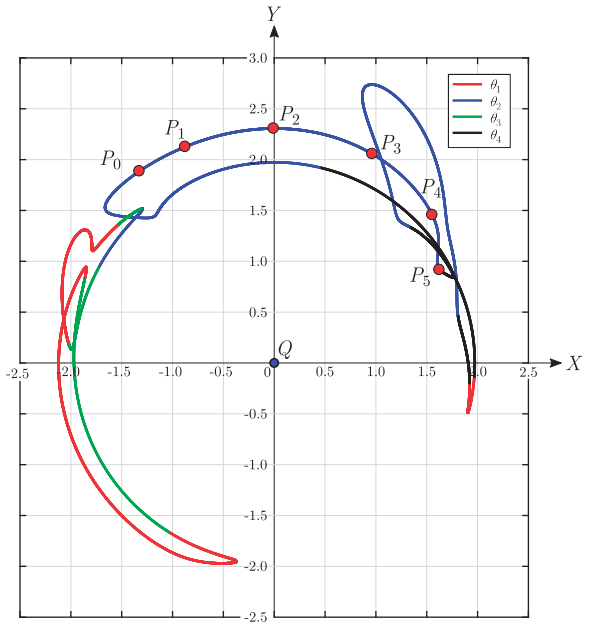

Figure 10. Trajectory of point *P* for the first example.

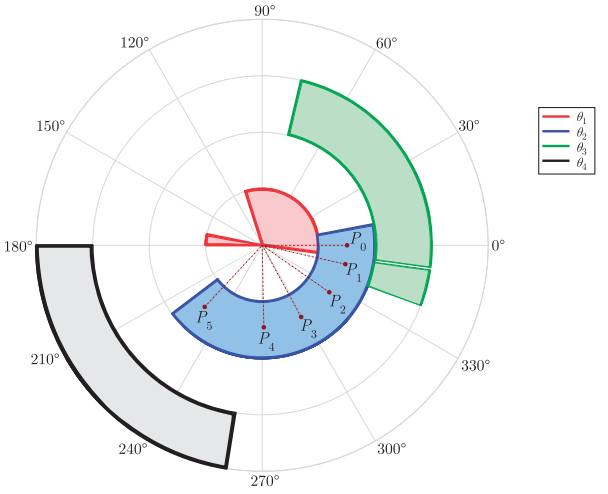

Figure 11. Solution regions associated with angle θ, first example.

Table 6. Design parameters for the second example.

Parameter	Numerical value	Parameter	Numerical value
x_B	1.7931	x_M	0.3259
y_B	−0.0273	y_M	2.0997
x_C	1.2916	x_N	−1.3909
y_C	−1.0358	y_N	−1.7500
x_Q	1.5249	e	2.3850
y_Q	−1.5556	f	1.1688
θ_0	0.0000°	L_{AP}	2.0000
a	−1.5284	δ	240°
b	0.2333	g	1.8000
L_{MR}	1.1179	L_{NS}	1.8230

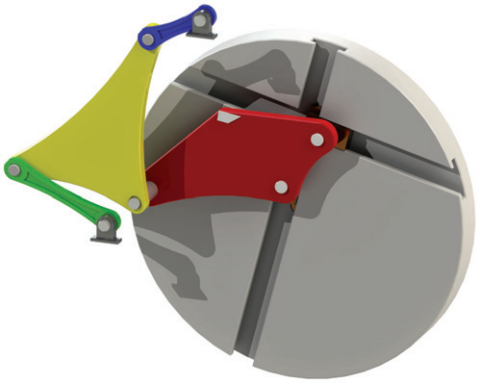

Figure 12. Resulting linkage for the second example.

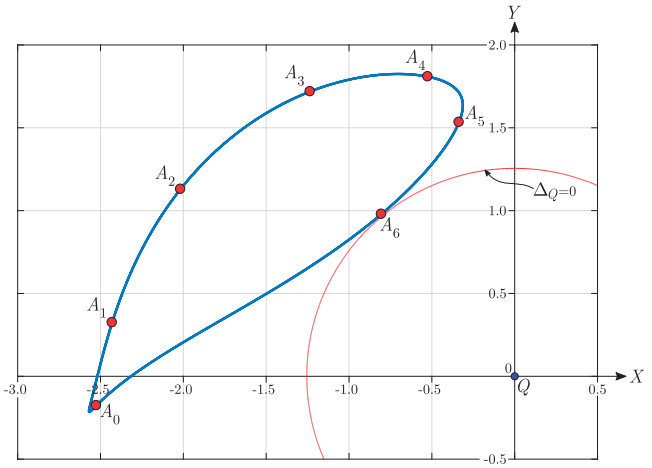

Figure 13. Coupler curve of the four-bar linkage for the second example.

algorithm shown in Table 3 leads to the design parameters presented in Table 6. A 3D layout of the resulting linkage is shown in Fig. 12.

The maximum synthesis error (round-off error) in this second example is 4.2×10^{-8} for the position of point P, and 2.5×10^{-6} degrees in the orientation of the guided body.

9.2.1. Evaluation of the performance of the second example

A careful analysis of Figs. 13–15, shows that the resulting linkage is free of branch and order defect, and it can move continuously between all the desired poses without disassembly. Therefore, this is a successful design.

9.3. Third example

This example addresses the design of a modified Wanzer linkage to visit exactly eight poses, see Table 4. Application of the computational algorithm shown in Table 3 leads to the design parameters presented in Table 7. A 3D layout of the resulting linkage is shown in Fig. 16.

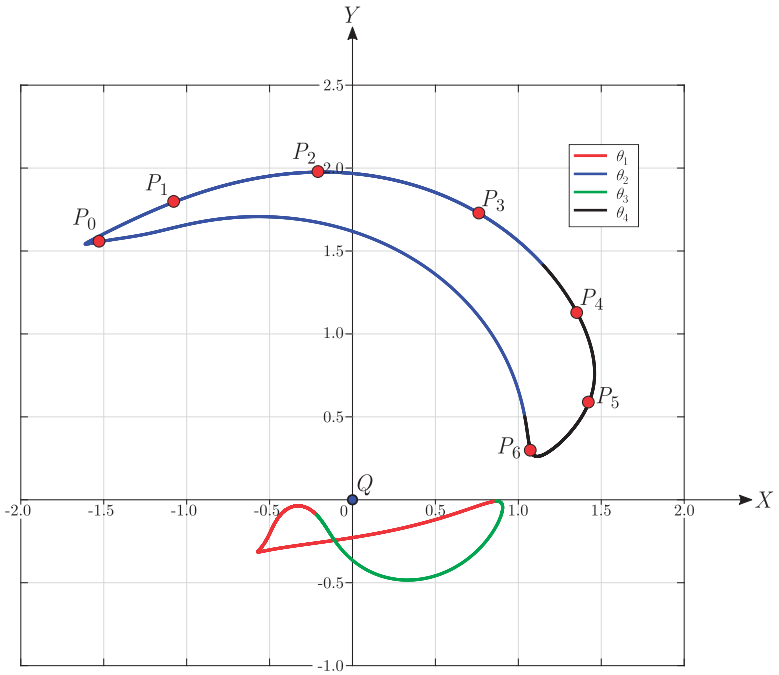

Figure 14. Trajectory of point *P* for the second example.

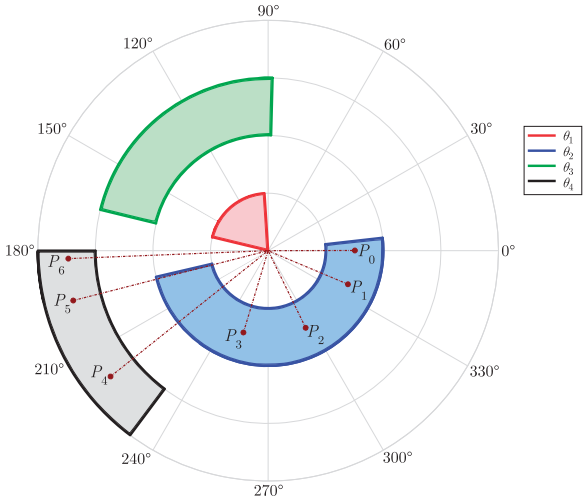

Figure 15. Solution regions associated with angle θ, second example.

The maximum synthesis error (round-off error) in this third example is 9.5×10^{-6} for the position of point *P*, and 6.7×10^{-4} degrees in the orientation of the guided body.

9.3.1. Evaluation of the performance of the third example

Based on the information shown in Figs. 17–19, it can be concluded that the resulting linkage is not free of branch defect, it will satisfy specified poses at isolated configurations, and it cannot move continuously between all the desired poses without disassembly. Therefore, this is an useful design for academic purposes only.

Table 7. Design parameters for the third example

Parameter	Numerical value	Parameter	Numerical value
x_B	−1.0555	x_M	2.4618
y_B	−3.1004	y_M	2.6287
x_C	3.6548	x_N	6.3114
y_C	−0.7435	y_N	−6.8307
x_Q	3.5231	e	2.8766
y_Q	−3.3015	f	0.2351
θ_0	−2.8999°	L_{AP}	2.0000
a	0.0306	δ	240°
b	−0.0023	g	2.2857
L_{MR}	2.1484	L_{NS}	10.5636

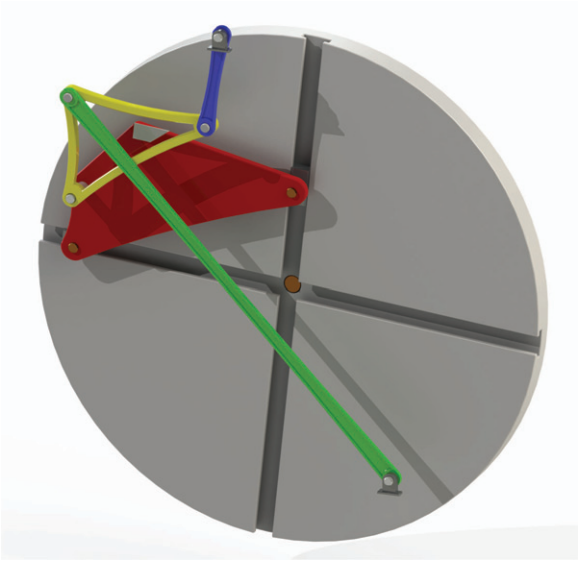

Figure 16. Resulting linkage for the third example.

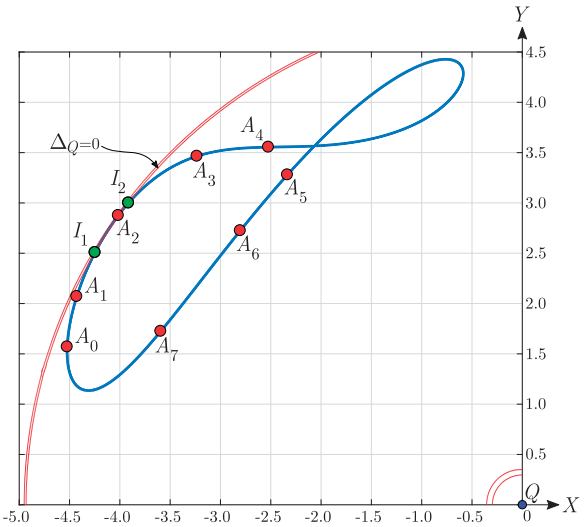

Figure 17. Coupler curve of the four-bar linkage for the third example.

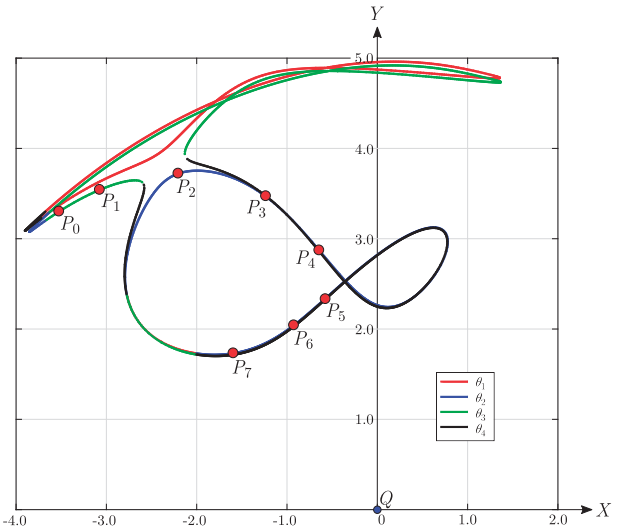

Figure 18. Trajectory of point *P* for the third example.

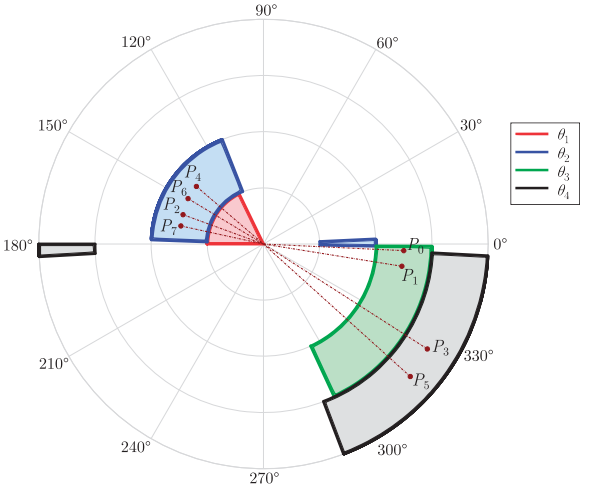

Figure 19. Solution regions associated with angle θ, third example.

10. Conclusions

The kinematic synthesis of linkages with advanced motion capabilities is a challenging task that deserves the attention of researchers. On this regard, this article contributed on the following aspects:

1. There has been introduced a novel planar linkage with advanced motion capabilities: the modified Wanzer linkage. It has one DOF and is able to reach up to eight poses on a plane.
2. A simple synthesis approach was presented, which lends itself to the construction of a systematic computational algorithm.
3. It has been developed an useful procedure for the identification of circuit, branch, and order defects of the design candidates.
4. For six and seven given poses, the synthesized linkages are free of branch and order defect, and they can move continuously between all the desired poses without disassembly. Therefore, they can be considered as successful designs.

5. The usefulness and the applicability of the proposed synthesis approach have been illustrated with three representative case studies.

It is expected that the different concepts addressed in this article may serve also to provide some useful guidelines to the design of new planar linkages with advanced motion capabilities.

Funding

This work was supported by the National Council of Science and Technology (CONACYT) of México, through SNI fellowships and scholarships.

References

Akgün, Y. (2016). A proposal for a convertible stadium roof structure derived from watt-I linkage. *Mechanics Based Design of Structures and Machines* 45:271–279. doi:10.1080/15397734.2016.1165117

Angeles, J., Bai, S. (2005). Some special cases of the Burmester problem for four and five poses. *International design engineering technical conferences & computers and information in engineering conference*. 24th–28th Sept. 2005. Long Beach, CA.

Bai, S. (2014). Dimensional synthesis of six-bar linkages with incomplete data set. Proceedings 5th European conference on mechanism science. 16th–20th Sept. 2014. Guimarães, Portugal.

Beyer, W. H. (1991). *Standard mathematical tables and formulae*. 29th ed. Boca Raton, FL: CRC Press, 12.

Brunnthaler, K., Pfurner, M., Husty, M. (2006). Synthesis of planar four-bar mechanisms. *Transactions of the Canadian society for mechanical engineering* 30(2):297.

Burnside, W., Panton, S. A. W. (1886). *Theory of equations*. Dublin, Irlanda: Dublin University Press, 142.

Chase, T. R., Mirth, J. A. (1993). Circuits and branches of single-degree-of-freedom planar linkages. *Journal of Mechanical Design* 115(2):223–30. doi:10.1115/1.2919181

Chen, C., Angeles, J. (2008). A novel family of linkages for advanced motion synthesis. *Mechanism and Machine Theory* 43(7):882–890. doi:10.1016/j.mechmachtheory.2007.06.007

Ge, Q., Zhao, J., Purwar., P. A. (2013). Decomposition of planar burmester problems using kinematic mapping. In: Vijay Kumar., ed. *Advances in mechanisms, robotics and design education and research*. Heidelberg, Germany: Springer International Publishing, 145–157. ISBN: 978-3-319-00398-6. doi:10.1007/978-3-319-00398-6_11

Gezgin, E., Chang, P. H., Akhan, A. F. (2016). Synthesis of a watt II six-Bar linkage in the design of a hand rehabilitation robot. *Mechanism and Machine Theory* 104:177–89. doi:10.1016/j.mechmachtheory.2016.05.023

Kohli, D., Cheng, J. C., Tsai, K. Y. (1994). Assemblability, circuits, branches, locking positions, and rotatability of input links of mechanisms with four closures. *Journal of Mechanical Design* 116(1):92–98. doi:10.1115/1.2919383

Kumar, G. A., Ganesan, G., Sekar, M. (2017). Near perfect path generation of cornerschamfered-rectangle and single synthesis cam-link mechanism to generate special-slot path. *Mechanics Based Design of Structures and Machines* 46:483–498. doi:10.1080/15397734.2017.1362565

McCarthy, J. M. (2002). *Design challenge to visit exactly 11 poses on a plane. Public communication.* ASME Design Engineering Technical Conferences.

Plecnik, M. M., McCarthy, J. M. (2016). Design of stephenson linkages that guide a point along a specified trajectory. *Mechanism and Machine Theory* 96(1):38–51. doi:j.mechmachtheory.2015.08.015

Balli, S., Chand, S. (2002). Defects in link mechanisms and solution rectification. *Mechanism and Machine Theory* 37(9):851–876. doi:10.1016/S0094-114X(02)00035-6

Sancibrian, R., de Juan, A., Sedano, A., Iglesias, M., Garcia, P., Viadero, F., Fernandez, A. (2012). Optimal dimensional synthesis of linkages using exact jacobian determination in the SQP algorithm. *Mechanics Based Design of Structures and Machines* 40(4):469–486. doi:10.1080/15397734.2012.687303

Schreiber, H., Meer, K., Schmitt, B. J. (2002). Dimensional synthesis of planar Stephenson mechanisms for motion generation using circle point search and homotopy methods. *Mechanism and Machine Theory* 37(7):717–37. ISSN: 0094-114X. doi:10.1016/S0094-114X(02)00016-2

Schröcker, H. P., Husty, M., McCarthy, J. M. (2005). Kinematic mapping based evaluation of assembly modes for planar four-bar synthesis. *ASME 2005 international design engineering technical conferences*. 24th–28th Sept. 2005. Long Beach, CA. EE.UU. doi:10.1115/DETC2005-85037

Soh, G. S., McCarthy, J. M. (2008). The synthesis of six-Bar linkages as constrained planar 3R chains. *Mechanism and Machine Theory* 43(2):160–170. doi:10.1016/j.mechmachtheory.2007.02.004

Suárez-Velásquez, H. A. (2018). *Exact synthesis of a modified Wanzer linkage to visit eight poses on a plane*. Spanish MA thesis, Universidad de Guanajuato.

Suh, C. H. C., Radcliffe, W. (1978). *Kinematics and mechanisms design*. Malabar, FL: Krieger Pub Co.

Uicker, J. J. G., Pennock, R. J., Shigley, E. (2017). *Theory of machines and mechanisms*. 5th ed. Cary, NC: Oxford University Press. ISBN: 9780190264482.

Venkataramanujam, V. P., Larochelle, M. (2015). Design and development of planar reconfigurable motion generators. *Mechanics Based Design of Structures and Machines* 44:426–439. doi:10.1080/15397734.2015.1096794